Non-Parametric Functional Muscle Network as a Robust Biomarker of Fatigue

Rory O'Keeffe, *Student Member, IEEE*, Seyed Yahya Shirazi, *Member, IEEE*, Jinghui Yang, Sarmad Mehrdad, *Graduate Student Member, IEEE*, Smita Rao, and S. Farokh Atashzar, *Senior Member, IEEE*

***Abstract*—Characterization of fatigue using surface electromyography (sEMG) data has been motivated for rehabilitation and injury-preventative technologies. Current sEMG-based models of fatigue are limited due to (a) linear and parametric assumptions, (b) lack of a holistic neurophysiological view, and (c) complex and heterogeneous responses. This paper proposes and validates a data-driven non-parametric functional muscle network analysis to reliably characterize fatigue-related changes in synergistic muscle coordination and distribution of neural drive at the peripheral level. The proposed approach was tested on data collected in this study from the lower extremities of 26 asymptomatic volunteers (13 subjects were assigned to the fatigue intervention group, and 13 age/gender-matched subjects were assigned to the control group). Volitional fatigue was induced in the intervention group by moderate-intensity unilateral leg press exercises. The proposed non-parametric functional muscle network demonstrated a consistent decrease in connectivity after the fatigue intervention, as indicated by network degree, weighted clustering coefficient (WCC), and global efficiency. The graph metrics displayed consistent and significant decreases at the group level, individual subject level, and individual muscle level. For the first time, this paper proposed a non-parametric functional muscle network and highlighted the corresponding potential as a sensitive biomarker of fatigue with superior performance to conventional spectrotemporal measures.**

***Index Terms*—Fatigue, functional muscle connectivity, network analysis, surface electromyography.**

Manuscript received 16 May 2022; revised 8 December 2022; accepted 27 December 2022. Date of publication 20 January 2023; date of current version 5 April 2023. This work was supported in part by the US National Science Foundation under Award #2229697 and Award #2037878. The work of Smita Rao was supported in part by the Foundation for Physical Therapy Research through Georgeny High Priority Award and in part by the NIH under Grant R01AR079182 and Grant R01DK114428. *(Seyed Yahya Shirazi and Jinghui Yang share the second authorship.) (Corresponding author: S. Farokh Atashzar.)*

Rory O'Keeffe, Seyed Yahya Shirazi, and Sarmad Mehrdad are with the Department of Electrical and Computer Engineering, New York University (NYU), New York, NY 11201 USA (e-mail: rok223@nyu.edu; sy.shirazi@nyu.edu; sm9167@nyu.edu).

Jinghui Yang is with the Department of Physical Therapy, New York, NY 10010 USA (e-mail: jy2796@nyu.edu).

Smita Rao is with the Department of Physical Therapy, New York University (NYU), New York, NY 10010 USA, also with the Department of Orthopedic Surgery, New York University Grossman, New York, NY 10016 USA, and also with the Department of Biomedical Engineering, NYU Tandon, Brooklyn, NY 11201 USA (e-mail: smita.rao@nyu.edu).

S. Farokh Atashzar is with the Department of Electrical and Computer Engineering, New York University (NYU), Brooklyn, NY 11201 USA, also with the Department of Mechanical and Aerospace Engineering at NYU, Brooklyn, NY 11201 USA, and also with NYU WIRELESS Center and NYU Center for Urban Sciences and Progress (CUSP), Brooklyn, NY 11201 USA (e-mail: f.atashzar@nyu.edu).

Digital Object Identifier 10.1109/JBHI.2023.3234960

I. Introduction

MUSCLE fatigue has been correlated with a degradation in the ability of a group of muscles to generate forces in response to the corresponding neural drive due to the changes in conduction fiber velocity, changes in recruitment patterns of motor units (especially fast units), and time synchronization in motor unit action potentials [1], [2], [3]. In the literature, fatigue is seen as a physiological phenomenon with a complex effect on human manipulability and mobility [4], [5], [6]. For example, fatigue has been postulated to drive muscle adaptation [7], exercise-induced hypoalgesia [8], while it can also challenge motor control and task completion, and consequently has been identified as a contributor to injury [9], [10], [11], [12]. Individuals with motor impairments secondary to neurological (such as stroke) and or orthopedic (such as knee ligament repair) conditions may experience altered patterns of muscle fatigue, likely because muscle recruitment also changes with these conditions [13], [14], [15]. Because of the above-mentioned reasons, it is important to objectively quantify and track fatigue and this can be used for injury prevention or monitoring the course of a rehabilitation regimen.

It is known that central motor control of the peripheral nervous system is critically responsive to muscle fatigue [16], [17], [18]. Muscle fatigue is accompanied by changes in muscle activation [19], conduction fiber velocities [20], [21], varied cocontraction patterns [22] and likely modulation of contralateral limb muscle activation either as a compensatory mechanism or due to the neurophysiological and biochemical interlinkage [23], [24], [25].

Surface electromyography (sEMG) has been historically used for fatigue analysis to capture potential changes in the exercised muscles. Although, sEMG has been seen as an informative modality for fatigue assessment, there is an extensive yet heterogeneous literature regarding the use of sEMG for fatigue monitoring [26], [27] and it is known that sEMG behavior is complex and often non-linear in response to fatigue [28], [29], [30].

In this regard, it was classically suggested that changes in motor unit recruitment and firing rate, caused by fatigue, can be seen as a decrease in median frequency (MDF) of sEMG

signals [31]. Also changes in magnitude activation, caused by fatigue may be seen as an increase in root mean square (RMS) of sEMG [32]. However, as mentioned earlier, due to the complexity of the sEMG in response to fatigue [28], the aforementioned observations are not always consistent. The RMS has been shown to both increase and decrease in response to fatigue during static and dynamic tasks [20], [33], [34], [35], [36], [37]. Indeed the RMS behavior was shown to vary depending on the fatiguing task protocol [38], [39]. The response of the MDF also varies depending on the protocol, with some studies reporting a decrease [20], [40], [41] and others observing no change [33], [42], [43]. In addition to the above, it can be mentioned that sEMG outcomes that focus on a single muscle behavior may be overly simplistic because fatigue-related changes are not only confined to the exercised muscle due to its holistic and systematic effect [7], [44].

As a result of the above-mentioned complexity of sEMG response to fatigue and inconsistency in the corresponding literature, more advanced modeling and analysis have been considered in the literature in order to explain, predict, or model fatigue [45], [46], [47], [48]. For example, muscle synergies have been discussed in the context of fatigue [49], [50], [51]. However, the literature suggests that synergy-based patterns are user-specific (depending on their recruitment history), and thus it may not be used as a consistent modeling technique for fatigue due to its high intersubject variabilities [52], [53], [54], [55], [56]. Thus, although synergy-based analysis may unfold some of the complexities in modeling fatigue, it may not be used as a robust, reliable, and reproducible method to monitor and model fatigue.

The above-mentioned discussion highlights the necessity of designing a novel method that can potentially provide a generalizable observation for a consistent group-level analysis besides individual-level monitoring as a trustworthy "biomarker". This motivates the current article, which proposes the use of a novel analysis, i.e., non-parametric muscle network.

In this regard, it should be noted that the discriminative power of functional connectivity networks based on bio-signals such as the electrohysterogram to distinguish physiological states (not including fatigue) has been recently demonstrated [57], [58]. In addition, the generic concept of functional muscle connectivity network has attracted a great deal of interest in the last five years as it can leverage full-spectrum synchronicity of muscle recruitment during functional tasks [59], [60]. In this regard, it should be noted that muscle networks reflect characteristics of both peripheral and central nervous systems in conduction of functional tasks, as it can quantify how the neural drive (generated by the central nervous system) is propagated among various groups of muscles which are recruited to conduct a functional task. This concept has been recently investigated, using linear spectral coherence analysis for non-fatiguing regular tasks, and shown high sensitivity to subtle motor changes [59], [61], [62], motivating the current study. Specifically, using intermuscular coherence, it is shown that muscle networks have high responsiveness to motor changes in the beta and gamma bands [59], [61]. It should be noted that such a level of task sensitivity to changes in motor tasks has not been reported before using muscle synergy analysis (which utilizes mainly sEMG envelopes) or other forms of conventional spectrotemporal metrics. To the best of our knowledge, the response of muscle networks to fatigue has not been evaluated in the literature.

It should also be noted that despite the aforementioned strength of functional muscle network analysis, all existing literature on functional muscle networks has been built based on conventional intermuscular coherence analysis (as the main processing method), which is a linear connectivity metric. Recently, the change of coherence in response to fatigue was found to be inconsistent across muscles [63], [64]. The inconsistent response could be due to limitations of the linear metric for capturing non-linear physiological changes.

Thus, in this paper, for the first time, we propose a non-parametric and non-linear holistic analysis of muscle network (designed to model monotonic but non-linear synchronicity in the activations of muscles) with the goal of providing a consistent understanding of the neurophysiological changes caused by fatigue. This paper hypothesizes that physiological fatigue can be readily quantified by a non-parametric form of intermuscular connectivity (Fig. 1). Unlike conventional connectivity metrics which are linear, such as Pearson's correlation or coherence, a non-parametric technique can detect more complex changes in the distributed peripheral nervous activities and is hence proposed in this work (Fig. 1(d)).

It should be noted that the protocol in this study quantifies non-parametric functional muscle network changes in a sit-to-stand task following a fatiguing leg press task. The leg press exercise would mostly fatigue muscles which control knee extension, including quadriceps muscles such as rectus femoris (RF) and vastus lateralis (VL) [65], [66]. Therefore, we further hypothesize that the greatest changes in the non-parametric muscle network will be noted in the RF and VL nodes of the network during the sit-to-stand task. The choice of the sit-to-stand task is supported by previous works, which have shown this task to be a useful test of composite lower extremity muscle strength [67], [68] in which knee extension is an important component [69], [70]. Sit-to-stand has also been utilized in clinical settings [71], [72], [73], and hence results from this work could potentially be applied to identifying fatigue during rehabilitation programs.

Given the uncovered potential of the non-parametric muscle network to measure variation in motor control after fatigue, metrics which quantify the network characteristics are utilized to analyze the consistency of network changes among 13 subjects. In this regard, the network's functional integration and segregation are considered as core characteristics which can evaluate changes in the collective neural drive due to fatigue, and are quantified using global efficiency (GE), degree and weighted clustering coefficient (WCC) respectively (definitions of GE, degree, and WCC can be found in [74], [75]).

In this paper, we investigated the effect of targeted fatigue on the non-parametric synchronicity between lower limb muscles. Lower extremity sEMG was assessed in thirteen asymptomatic volunteers during 30 s of a sit-to-stand task, performed before and after completing a fatiguing task. Separately, the protocol was repeated with an age/gender-matched control group of thirteen asymptomatic participants, but the fatiguing task was removed (in order to isolate the effect of fatigue). With fatigue, the non-parametric muscle network demonstrated a consistent decrease in graph-based metrics (in particular, network degree, WCC, and global efficiency) at the group and individual subject levels. Without fatigue, the results of the control group showed an absence of consistent network changes between trials of sit-to-stand. The control group results highlighted the reliability of the proposed muscle network metrics and isolated the effect

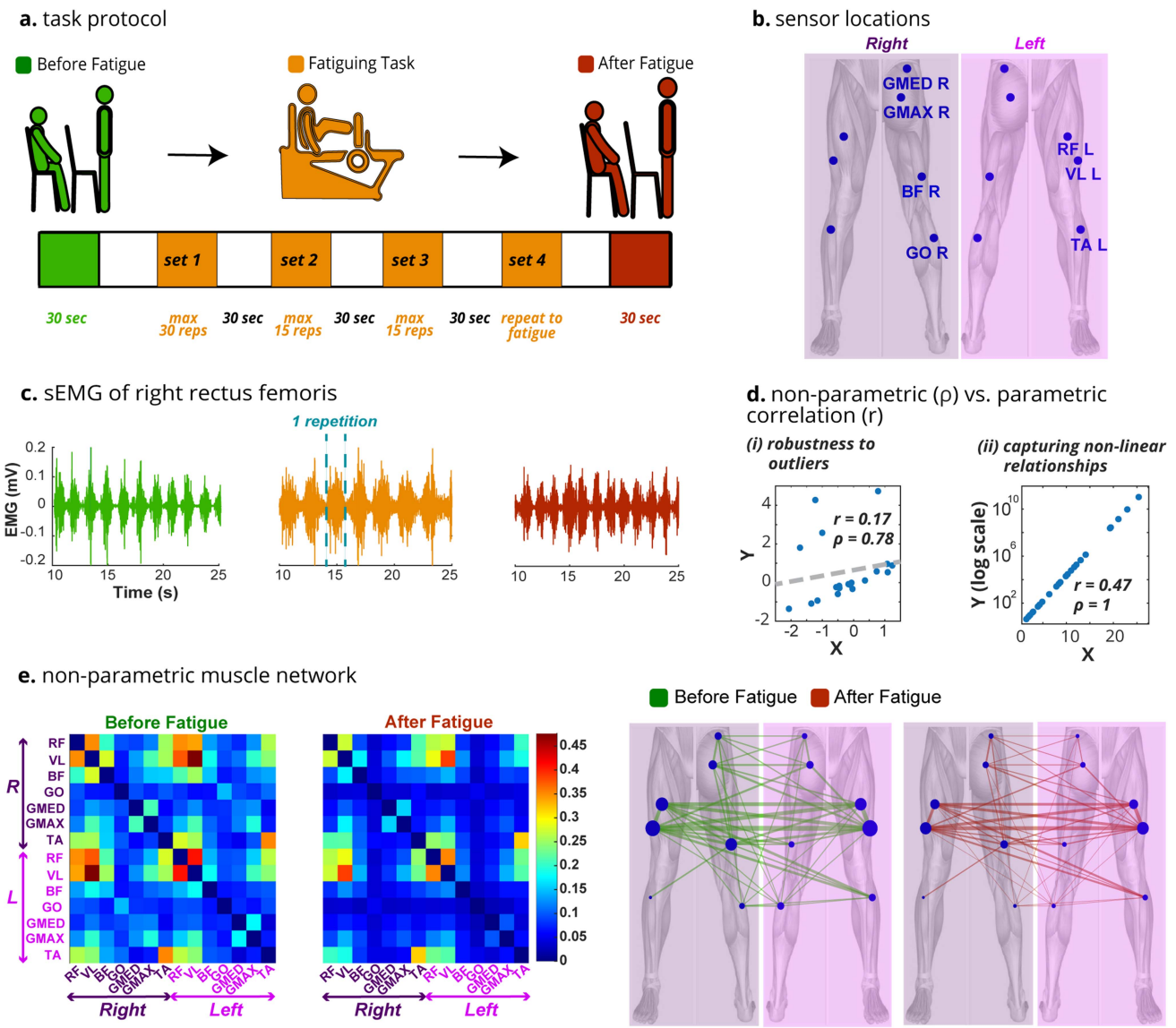

Fig. 1. Experimental Outline. **a.** Subjects performed 30 s of sit-to-stand repetitions before and after a fatiguing task. The fatiguing task consisted of four sets of resistance exercises with a leg press machine. **b.** Seven bipolar sEMG sensors were placed bilaterally on the anterior and posterior leg muscles. GMED = Gluteus Medius, GMAX = Gluteus Maximus, BF = Biceps Femoris, GO = Gastrocnemius, RF = Rectus Femoris, VL = Vastus Lateralis, TA = Tibialis Anterior. **c.** An exemplar sEMG recording from RF during the sit-to-stand pre-fatigue, fatiguing exercise and sit-to-stand post-fatigue. **d.** (i) Spearman power correlation (ρ) is **non-parametric** and more robust than the parametric Pearson correlation (r) to outliers. The grey dashed line corresponds to the least squares linear regression (which is skewed by the outliers, $r^2 = 0.22$). (ii) ρ captures non-linear relationships such as an exponential function while the linear Pearson correlation (r) cannot accurately measure the monotonic correlation. **e.** Subject-mean non-parametric muscle network. Spearman power correlation (ρ_{xy}) was computed between all muscle pairs to generate the non-parametric muscle network. The heat map (left) illustrates the changes from before to after for all network edges. The top 50% most changeable edges from before to after fatigue are shown in the network map (right). The width of the lines is proportional to the ρ_{xy} between that muscle pair and the size of the circles is proportional to the degree of that node (muscle). The mean network comparison highlights the stronger connectivity trends before versus after fatigue.

of fatigue observed in the intervention group. The results suggest that the proposed non-parametric muscle network can be an effective and robust biomarker of fatigue.

II. Methods

A. Fatigue Intervention

Thirteen asymptomatic subjects (seven females, six males) with an age of 26.0 ± 3.7 (mean ± standard deviation (SD)) years and a BMI of 22.7 ± 3.2 (mean ± SD) kg.m^2 participated in the fatigue intervention study. The institutional review board of New York University approved the study (IRB-FY2019-3039), and subjects provided their written consent after they received the study description. Following the institutional review board approval, individuals between 18-50 years old who had no pain at the time of the study were recruited. Note that the actual age range of recruited subjects was 19-32 years. Individuals who were bedridden for more than three days, had major surgery within the last 12 weeks, had been diagnosed with cancer in

TABLE I
LEG PRESS INFORMATION OF SUBJECTS

Subject	Set # 1	Set #2	Set #3	Set #4	Load (lbs)
1	30	15	12	11	20
2	30	15	15	15	100
3	30	15	15	15	100
4	30	15	15	15	30
5	30	15	12	12	100
6	27	12	9	7	15
7	30	15	10	7	100
8	13	12	10	8	40
9	30	15	15	15	20
10	24	15	10	9	100
11	25	15	11	14	60
12	30	15	15	15	45
13	30	15	15	15	30
mean	27.62	14.54	12.62	12.1	58.46
SD	4.87	1.13	2.43	3.34	36.08

TABLE II
SIT-TO-STAND REPETITIONS, BEFORE AND AFTER FATIGUE

Subject	Before	After
1	22	20
2	21	24
3	11	11
4	10	11
5	29	32
6	7	7
7	10	12
8	8	7
9	10	11
10	15	21
11	8	8
12	10	8
13	7	8
mean	12.92	13.85
SD	6.87	7.88

the last six months, or had any conditions related to sensory or musculoskeletal dysfunction were not recruited. If a subject was physically unable to complete the protocol on the day of the experiment, they were excluded.

1) Experimental Procedure: Subjects performed a sit-to-stand task before and after sub-maximal fatigue was induced by a single-session of moderate intensity resistance exercise (Fig. 1(a)). The 30 s sit-to-stand task involved repeatedly standing up from a seated position in a chair, for 30 seconds [76], [77]. Next, one repetition maximum (1RM) was determined for the unilateral leg press. Subjects then performed four sets at 50% of the 1RM on their right side, with a target of 30 repetitions in the first set and a target of 15 repetitions for the last three sets to induce sub-maximal fatigue [78], [79]. The last set was specifically performed to failure, defined as the inability to complete a repetition while maintaining cadence and form. The load with which the leg press was performed in addition to the mean and SD number of repetitions for each set are shown in Table I. Subjects were given a fixed recovery time (30 seconds) between sets. All participants reported an RPE (Rate of Perceived Exertion) of 18 at the final repetition. Ninety seconds after completing the last repetition of the leg press, subjects performed the post-fatigue sit-to-stand task. Subjects were instructed to complete the sit-to-stand at a natural rate and the number of repetitions was recorded. As illustrated in Table II, the number of repetitions was comparable before and after fatigue, for all subjects.

sEMG signals were recorded from fourteen sensors (Fig. 1(b)), using the wireless Trigno sEMG system (Delsys Inc., Natick, MA), with a sampling frequency of 1259 Hz and a built-in 20 Hz high-pass filter. Fourteen bipolar Trigno Avanti sensors were used bilaterally for (i) Rectus Femoris (RF), (ii) Vastus Lateralis (VL), (iii) Tibialis Anterior (TA), (iv) Gluteus Medius (GMED), (v) Gluteus Maximus (GMAX), (vi) Biceps Femoris (BF) and (vii) Gastrocnemius (GO). The skin surface was thoroughly wiped prior to sensor placement. Sensors were placed parallel to the direction of the muscles. Following the recording, signals were pre-processed using MATLAB R2020b (MathWorks Inc., Natick, MA). The first and last one second of all trials were clipped out.

2) Non-Parametric Muscle Network: A zero-phase Butterworth low pass filter was applied at 50 Hz, such that the resultant sEMG signals were in the 20–50 Hz range. This range was chosen since recent work has shown that humans reorganize coherence-based muscle networks across limbs in the beta-to-gamma bands [59]. Spearman power correlation networks were constructed for before and after fatigue since it is robust to outliers and can capture non-linear monotonic relationships (Fig. 1(d)).

Spearman power correlation (ρ_{xy}) between two sEMG signals $x(t)$ and $y(t)$ was computed. The power time series $x^2(t), y^2(t)$ were first calculated and then each power time series was rank transformed. For example, an sEMG signal with n samples will have its power values replaced by ranks from 1 to n, in ascending order - the maximum power value will be assigned the rank n. The power time series $x^2(t)$ and $y^2(t)$ were rank transformed to $p_x(t)$ and $p_y(t)$ respectively, and the respective means $\bar{p}_x$ and $\bar{p}_y$ across the n samples were calculated. ρ_{xy} is computed according to:

$$\rho_{xy} = \frac{\sum_{t=1}^{n} \left(p_x(t) - \bar{p}_x\right)\left(p_y(t) - \bar{p}_y\right)}{\sqrt{\sum_{t=1}^{n} \left(p_x(t) - \bar{p}_x\right)^2 \sum_{t=1}^{n} \left(p_y(t) - \bar{p}_y\right)^2}} \quad (1)$$

For the muscle network, the magnitude $|\rho_{xy}|$ was computed between each sensor pair, across the sit-to-stand trial duration. When using the magnitude $|\rho_{xy}|$, the monotonic negative correlation between $x^2(t)$ and $y^2(t)$ of $-\rho_{xy}$ is interpreted as having equivalent non-parametric connectivity to the monotonic positive correlation of ρ_{xy}. Each node in the network represents a muscle, and the width of each line illustrates $|\rho_{xy}|$.

The degree of each node, D_i, is the average of all edges connected to the node. If the muscle network is represented by adjacency matrix A, D_i is defined as:

$$D_i = \left(\frac{1}{N-1}\right) \sum_{j=1, j\neq i}^{N} A_{ij}, \quad (2)$$

where N is the number of nodes and A_{ij} represents the edge that connects nodes i and j. Mean network degree, is the mean of all nodes' degrees:

$$\bar{D} = \frac{1}{N} \sum_{i=1}^{N} D_i \quad (3)$$

A node's weighted clustering coefficient (WCC_i) gives a relative measure of how well node i is connected to its neighbors (A_{ij}, A_{ik}) while also accounting for the neigbors' interconnection (A_{jk}). A node's clustering coefficient (CC_i) can be

considered the sum of the triangles ($\sum_i t_i$) connected to node i, normalized by the maximum possible value [80].

$$CC_i = \frac{2\sum_i t_i}{(N-1)(N-2)} \tag{4}$$

Each triangle's value will be the product of the three edges, $t_i = A_{ij}A_{ik}A_{jk}$. The weighted adjacency matrix $\tilde{A}$ is scaled by the maximum connection in the network, hence $\tilde{A}_{ij} = A_{ij}/\max(A)$. The node's weighted clustering coefficient WCC_i is then defined as:

$$WCC_i = \frac{2}{(N-1)(N-2)} \sum_{j,k} (\tilde{A}_{ij}\tilde{A}_{ik}\tilde{A}_{jk})^{(1/3)} \tag{5}$$

A node which has (i) 0 connectivity to its neighbors or (ii) has neighbors whose interconnections are all 0 will have $WCC_i = 0$, while a node which is (i) maximally connected to its neighbors and (ii) has neighbors whose interconnections are all maximal has $WCC_i = 1$. Note that the value of WCC_i is more dependent on node i's connections to its neighbors ($\tilde{A}_{ij}, \tilde{A}_{ik}$ terms) rather than the neighbors' interconnections ($\tilde{A}_{jk}$ term). Mean network WCC, is the mean of all nodes' WCCs:

$$\overline{WCC} = \frac{1}{N}\sum_{i=1}^{N} WCC_i \tag{6}$$

Global efficiency is directly proportional to how well the network is connected overall. The efficiency (E) of a network is defined as:

$$E = \frac{1}{N(N-1)} \sum_{i \neq j} \frac{1}{L_{ij}}. \tag{7}$$

where L_{ij} is the shortest path between nodes i and j [74], [81]. The efficiency (E) is normalized by the ideal efficiency (E_{id}) to give the global efficiency, GE:

$$GE = \frac{E}{E_{id}}, \tag{8}$$

which is bounded between 0 and 1. A network with perfect connectivity will have $GE = 1$, while one with no connectivity will have $GE = 0$.

3) Fatigue Propagation in Muscle Network: The contributions from each effect of fatigue to the overall change in $|\rho_{xy}|$ were quantified. The mean $|\rho_{xy}|$ for a sub-network within each subject's fourteen-muscle network was computed, and the bar plot illustrates the median across subjects (Fig. 5). The overall effect of fatigue is defined as the change in the mean $|\rho_{xy}|$ across the fourteen-muscle network (**All-All**). The primary effect type 1 is defined as the change in the $|\rho_{xy}|$ between RF and VL on the fatigue-targeted side (**RF-VL**). The primary effect type 2 is defined as the change in the mean of 13 $|\rho_{xy}|$ values between each fatigue-targeted muscle and other muscles (**RF-All** and **VL-All**). The secondary effect is defined as the change in the mean $|\rho_{xy}|$ across the twelve-muscle network without the fatigue-targeted muscles (**All-All without RF and VL**).

4) Conventional Spectrotemporal Measurements: To compare the proposed network results to the existing attempted biomarker methods, RMS, power spectral density (PSD) and median frequency (MDF) were computed for particular muscles. All measurements were calculated by considering the full trial duration, before and after fatigue, for each subject. For the calculation of RMS, PSD and MDF, the full sEMG bandwidth (20–200 Hz) was considered to minimize contamination of the sEMG signals by movement artifacts and analyze the most significant portion of the signals' power spectrum [82], [83], [84], [85]. The signal was band-pass filtered between 20 and 200 Hz with a zero-phase 4th order Butterworth filter in addition to applying zero-phase 4th order Butterworth notch filters (half-width = 2.5 Hz) at multiples of 60 Hz. For the purpose of RMS calculation, each trial's signal envelope (the magnitude of the Hilbert transform) was normalized. Normalization was performed because it reduces inter/intra-individual variability of the sEMG amplitude values based on recommendations from the literature [86], [87], [88], [89], [90]. For each muscle, the envelopes from all subject trials were concatenated before computing the ensemble mean. After dividing the trial envelope by the corresponding ensemble mean and thus normalizing with a method appropriate for the isotonic sit-to-stand task [91], [92], the normalized RMS was computed across the trial duration. The filtered signal without any normalization was used for PSD and MDF calculations. In the case of PSD, the median PSD in the 20–200 Hz range was used. The MDF is defined as that frequency which divides the area under the power spectrum density curve in two, hence it indicates the power spectrum shape while the median PSD indicates the overall magnitude. In Fig. 2(b), the mean for each of RMS (mean (RMS)), median PSD (mean (median PSD)), and MDF (mean (MDF)) was computed across fourteen muscles.

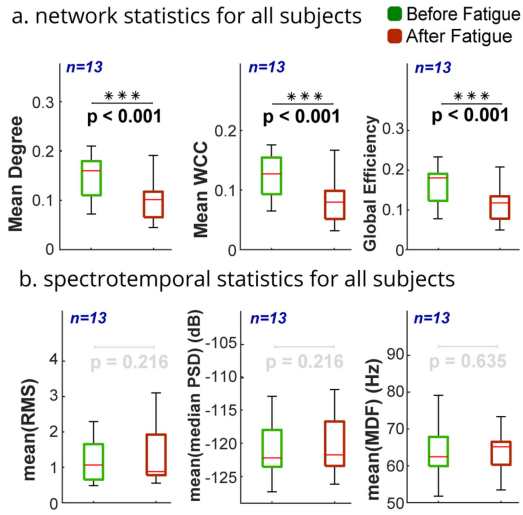

Fig. 2. Statistical analysis for all subjects. The effect was investigated by testing for statistical significance between the metrics' distributions before and after fatigue using the Wilcoxon signed-rank test. **a.** Mean degree, mean WCC and global efficiency are compared from before to after fatigue ($n = 13$ subjects). For all network metrics, the null hypothesis that the distributions are similar was rejected at the 0.05 significance level *(mean degree, mean WCC and global efficiency: $p < 0.001$.)* **b.** For each of mean (RMS), mean (median PSD), and mean (MDF), the Wilcoxon signed-rank test failed to reject the null hypothesis *(mean (RMS), mean (median PSD) and mean (MDF): $p > 0.215$).*

B. Control Group: Without Fatigue Intervention

The effect of the presence or absence of fatigue on changes in the non-parametric muscle network was investigated by repeating the protocol without the fatigue intervention. Thirteen control subjects (seven females, six males) with an age of 25.9 ± 4.3 (mean ± SD) years and a BMI of 22.9 ± 2.7 (mean

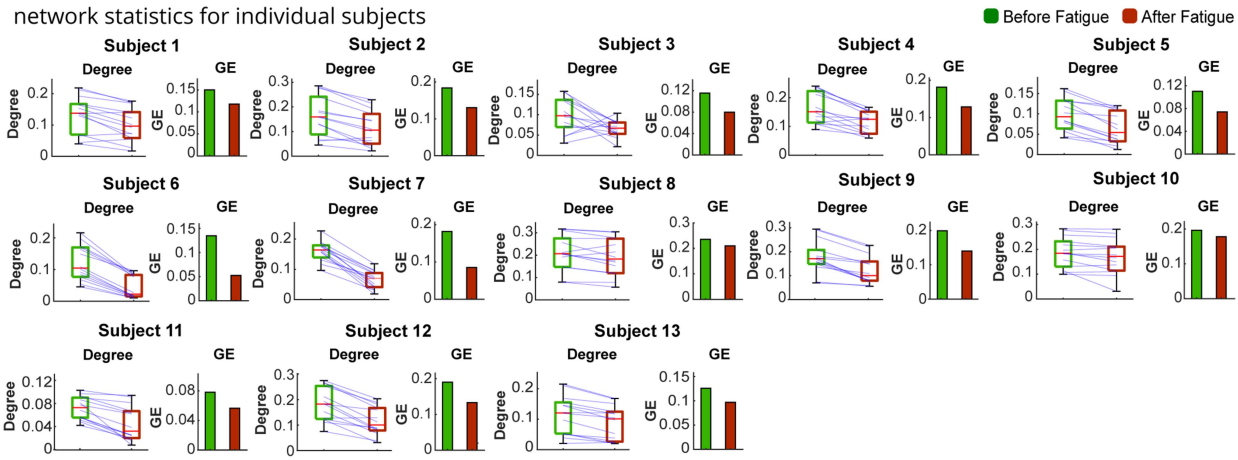

Fig. 3. Non-parametric muscle network statistics for each subject, comparing before and after fatigue. The degree for all fourteen nodes form the distributions and the blue hairlines depict the change in degree from before to after fatigue. The median degree and global efficiency (GE) decreased from before to after fatigue for 13/13 subjects.

TABLE III
CONTROL GROUP: SIT-TO-STAND REPETITIONS

Subject	Trial 1	Trial 2
14	12	13
15	15	17
16	10	9
17	8	9
18	11	11
19	21	19
20	10	10
21	8	9
22	19	17
23	8	9
24	25	24
25	8	11
26	12	13
Mean	12.85	13.15
Std	5.57	4.74

$\pm$ SD) kg.m^2 participated in the without-fatigue study. The institutional review board of New York University approved the study (IRB-FY2022-5888), and the inclusion/exclusion criteria matched those of the fatigue intervention study. The protocol, including time between tasks and task duration, was matched with the protocol of the fatigue intervention study, but the fatiguing task was removed. Subjects performed two 30-second trials of sit-to-stand separated by a rest interval while sEMG signals were recorded. The number of repetitions for each trial is shown in Table III.

C. Statistical Analysis

To evaluate the statistical trends observed in absolute power correlation muscle networks, (i) group-level, (ii) individual subject and (iii) particular node analyses were conducted. In all cases, connectivity ($|\rho_{xy}|$) was evaulated at each of the fourteen nodes. Group level analysis examines the change in mean degree, mean WCC and global efficiency distributions (Figs. 2(a), and 7) across all subjects ($n = 13$). Individual level analysis examines the change in each subject's network, specifically the degree of all nodes and global efficiency (Figs. 3, and 8). When considering the connectivity statistics of particular nodes (Fig. 4), the node's absolute power correlations for all subjects are included ($n = 13$). Similarly, when considering the spectrotemporal measurements (e.g. RMS in (Fig. 6)), a given muscle's value for all subjects ($n = 13$) is used for the statistical analysis.

The Kolmogorov-Smirnov test for normality rejected the normal distribution hypothesis for the absolute Spearman power correlation distributions (Figs. 2(a), 4, and 7). The Wilcoxon signed-rank test was used to test statistical significance, with the significance level $\alpha = 0.05$. For the sake of even comparison, the Wilcoxon signed-rank test was also utilized for measuring the significance of spectrotemporal measurement distributions (Fig. 6) and the response of the muscle network without fatigue (Figs. 7 and 8).

III. RESULTS

A. Response of Muscle Network to Fatigue

1) Group Analysis of Non-Parametric Muscle Network: The group-level results from the sit-to-stand task show a strong trend of decreasing lower limb network connectivity after fatigue. The subject-mean network (i.e., the mean network calculated by the average of each pairwise connection across all subjects) in both heat map and network map forms indicate this decreasing connectivity (Fig. 1(e)). To confirm these trends, graph theory metrics of connectivity (degree, WCC and global efficiency) were evaluated. Group-level statistical analysis of all subjects' network metrics confirms that non-parametric intermuscular connectivity significantly decreases from before to after fatigue (Fig. 2(a)). All network metrics were significantly higher before the fatiguing exercise than after (*mean degree, mean WCC and global efficiency:* $p < 0.001$). These results illustrate that the non-parametric muscle network can detect the effect of fatigue at the group level.

The effect of decreasing connectivity with fatigue appears to be most pronounced in quadriceps muscles (Fig 1(e)). We note the decrease in the size of the nodes (proportional to degree of the node) for the two quadricep muscles, i.e. RF and VL, in a bilateral manner. Looking at the heat maps, it appears that for the ipsilateral RF-VL connection on both sides, there is a marked decrease from before to after fatigue (Fig 1(e)). High connectivity was observed for contralateral muscle pairs, for example left RF with right RF, left VL with right VL. These

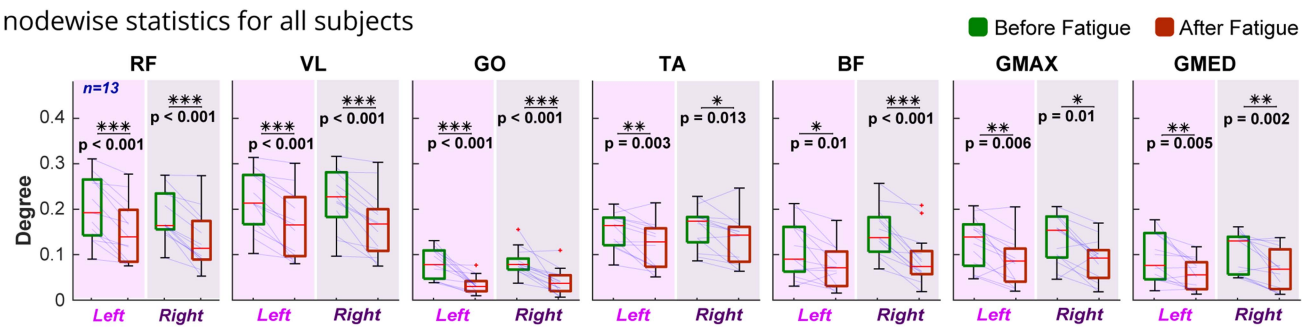

Fig. 4. Nodewise non-parametric connectivity statistics across all subjects, comparing before and after fatigue ($n = 13$). The blue lines show the change in degree from before to after fatigue for each subject. For all fourteen muscles, the degree of all subjects decreased from pre to post-fatigue (*Wilcoxon signed rank test* $p < 0.014$). The fatigue-induced decrease was most pronounced for RF bilaterally, VL bilaterally and right BF ($p < 0.001$ and 13/13 subjects followed the group trend).

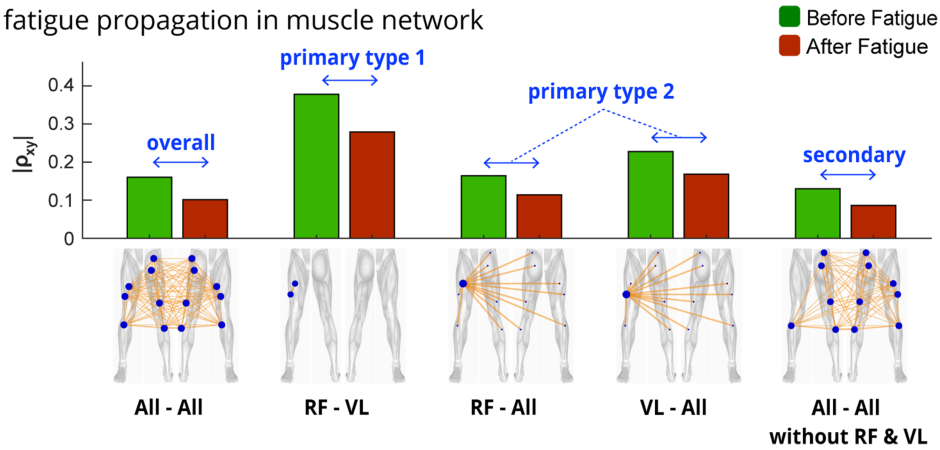

Fig. 5. Analysis of the contributions from each effect of fatigue to the overall decrease in $|\rho_{xy}|$. Each effect was estimated as the change in the mean $|\rho_{xy}|$ across a sub-network within each subject's fourteen-muscle network and the bars represent the median across subjects. All-All indicates the complete fourteen-muscle network, and the change in the mean $|\rho_{xy}|$ measures the overall effect of fatigue. RF-VL indicates the single $|\rho_{xy}|$ between the two fatigue-targeted muscles, and the change measures the primary effect type 1 of fatigue. RF-All and VL-All each indicate a sub-network composed of the thirteen connections between the fatigue-targeted and other muscles, and the change in the mean $|\rho_{xy}|$ measures the primary effect type 2 of fatigue. All-All without RF and VL indicates the twelve-muscle network without the fatigue-targeted muscles, and the change in the mean $|\rho_{xy}|$ measures the secondary effect of fatigue. The primary and secondary effects indicated a decrease in non-parametric connectivity which contributed to the overall post-fatigue decline.

two connections also appear to show a decrease after fatigue. The contralateral effect (for further detail see Discussion section, paragraph 5) highlights the possible systematic effect of fatigue on neural aspects of motor control.

In contrast to the overall network metrics, the mean of each spectrotemporal metric did not show a significant response to the effect of fatigue (Fig. 2(b)). For each of mean (RMS), mean (median PSD), and mean (MDF), the Wilcoxon signed-rank test failed to reject the null hypothesis *(mean (RMS), mean (median PSD) and mean (MDF):* $p > 0.215$*)*.

2) Individual Analysis of Non-Parametric Muscle Network: Non-parametric muscle network analysis was undertaken for each subject to explore the possibility of between-subject variability in pattern and extent of connectivity. All thirteen subjects showed a pattern of decreasing connectivity after fatigue, with a decrease in both degree and global efficiency (Fig. 3). The percentage change in global efficiency from before to after fatigue was calculated for each subject, and the mean percentage change across subjects was a decrease of 30% $\pm$ 14.6% (mean $\pm$ SD). This subject-specific result further emphasizes the robustness of the non-parametric muscle network's response to fatigue.

3) Nodewise Analysis of Non-Parametric Muscle Network: The non-parametric connectivity of all nodes (muscles) was analyzed (Fig. 4) and all left and right-side muscles showed a significant decrease in node degree from before to after fatigue ($p < 0.014$). The decrease was most pronounced for RF bilaterally, VL bilaterally and right BF ($p < 0.001$). This demonstrates that not only does the overall network show a significant decrease from before to after fatigue, individual nodes also exhibit the connectivity decline. Moreover, the blue hairlines show the individual subject changes and this most strongly emphasizes the robustness of the result for RF bilaterally, VL bilaterally and right BF since all subjects follow the group trend of decreasing connectivity.

4) Fatigue Propagation in Muscle Network: Each of the three effects of fatigue contributed to the overall decrease in non-parametric connectivity (Fig. 5). Examining the change in the

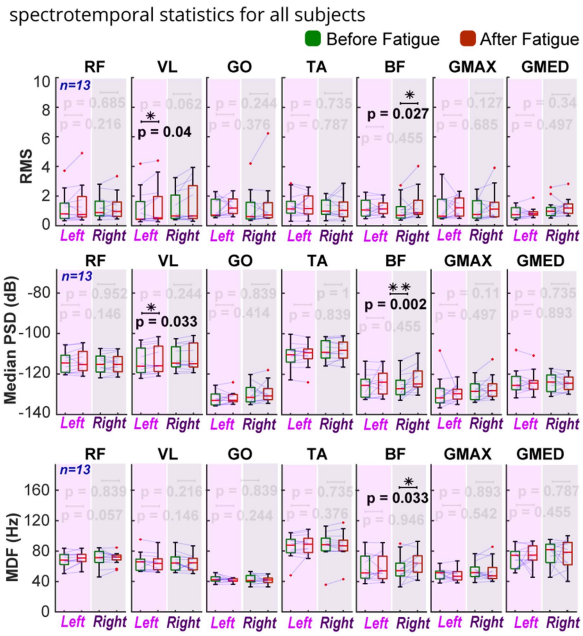

Fig. 6. Nodewise spectrotemporal measurements statistical analysis. Distributions are constructed for each muscle using all subject values for that measurement ($n = 13$). Blue hairlines show the individual subject changes. **a.** The change in RMS on both left and right is analyzed, before and after fatigue. Left VL ($p = 0.04$) and right BF ($p = 0.027$) each show a small increase. **b.** Change in PSD (median in 20–200 Hz range), before and after fatigue. Left VL ($p = 0.033$) and right BF ($p = 0.002$) show an increase. **c.** Change in MDF, before and after fatigue. Right BF shows an increase ($p = 0.033$).

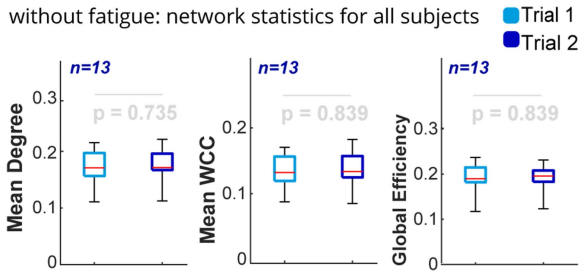

Fig. 7. Statistical analysis for all subjects, comparing the non-parametric muscle network changes between two trials of sit-to-stand, in the absence of fatigue. Mean degree, mean WCC and global efficiency are compared between the trials ($n = 13$ subjects). For all network metrics, the null hypothesis that the two trials have similar distributions was not rejected at the 0.05 significance level *(Wilcoxon signed-rank test for mean degree, mean WCC and global efficiency: $p > 0.734$).*

median across subjects, it was observed that, interestingly, all three effects showed a decrease which contributed to the overall decline in non-parametric connectivity post-fatigue.

5) Nodewise Analysis of Spectrotemporal Measurements: In contrast with the robust and consistent results obtained for the non-parametric intermuscular coupling in response to fatigue, classical sEMG-based spectrotemporal measurements of fatigue showed inconsistent responses. The RMS, PSD (median in 20–200 Hz range) and MDF for each muscle are shown in Fig. 6. There was a significant pairwise change in RMS and median PSD for left VL from before to after fatigue ($p = 0.041$) although the respective medians were almost equal. There was a significant post-fatigue increase in RMS, median PSD, and MDF for right BF ($p = 0.034$) although for each metric, the blue hairlines show that 2 or more subjects decreased contrary to the group trend (Fig. 6). Overall, there was a lack of a robust general trend across the subjects and muscles for the spectrotemporal metrics in contrast to the non-parametric muscle network results.

B. Response of Muscle Network Without Fatigue Intervention

1) Group Analysis of Non-Parametric Muscle Network: Group-level statistical analysis of all subjects' network metrics did not indicate a significant change in non-parametric connectivity from Trial 1 to Trial 2 without the fatigue intervention (*Wilcoxon signed-rank test for mean degree, mean WCC and global efficiency:* $p > 0.734$, Fig. 7).

2) Individual Analysis of Non-Parametric Muscle Network: Non-parametric muscle network analysis was undertaken for each subject to explore the possibility of between-subject variability in pattern and extent of connectivity. Analysis of the change in network metrics did not reveal either consistent increase or decrease from Trial 1 to Trial 2 (Fig. 8). Seven subjects increased while six subjects decreased their median degree and global efficiency from Trial 1 to Trial 2. The percentage change in global efficiency from Trial 1 to Trial 2 was calculated for each subject, and the mean percentage change across subjects was a decrease of $0.35\% \pm 5.4\%$ (mean $\pm$ SD).

IV. Discussion

The key findings of our study indicate that the non-parametric muscle network is a statistically robust biomarker of fatigue, since it efficiently delineated fatigue-related changes at the group and individual levels. Moreover, key muscles were shown to have a decrease in their degree for all subjects, emphasizing the ability of the network to detect degradation of the peripheral nervous system (PNS) response to central nervous system (CNS) command after resistance-training induced muscle fatigue. Additionally, conventional methods (RMS, PSD and MDF) showed heterogeneous responses to fatigue, highlighting the relative strength of the proposed method. The proposed method can be utilized in rehabilitation settings involving assessment and intervention, where sensitive and comprehensive quantification of fatigue is needed.

As hypothesized, the non-parametric muscle network was able to detect muscle fatigue. This is demonstrated by post-fatigue decreases in network metrics at the group (Fig. 2(a)) and individual (Fig. 3) levels. The absolute Spearman power correlation detects fatigue-related decreases in the non-parametric coupling between muscle activations (in power form), which is illustrated by the median degree and global efficiency declining for all subjects (Fig. 3). The ability of the proposed biomarker to detect the effect of neurophysiological changes associated with fatigue was indicated by, firstly, the consistent response of network metrics across a subject pool with a wide range of physical capabilities, and secondly, the failure of the classical measures to show a consistent behavior for the same pool of subjects in this study. The fatigue-related degradation in the non-parametric intermuscular coupling was highlighted in all seven muscles bilaterally (Fig. 4). In the control group, we did not observe consistent differences between Trial 1 and Trial 2 at the group (Fig. 7) or individual levels (Fig. 8). This observation highlights the reliability of the method in the absence of the

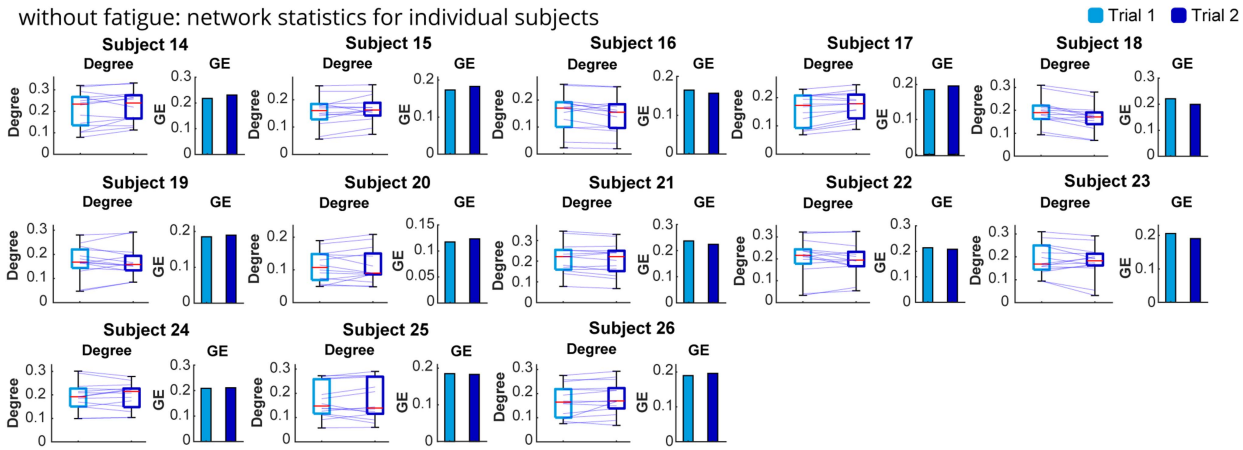

Fig. 8. Non-parametric muscle network statistics for each subject, comparing two trials of sit-to-stand, in the absence of fatigue. The degree for all fourteen nodes form the distributions and the blue hairlines depict the change in degree between the trials. Seven subjects increased while six subjects decreased their median degree and global efficiency from Trial 1 to Trial 2. The percentage change in global efficiency (GE) from Trial 1 to Trial 2 was calculated for each subject, and the mean percentage change across subjects was a decrease of 0.35% $\pm$ 5.4% (mean $\pm$ SD).

intervention, as well as the sensitivity to fatigue when comparing the control group results with the significant change in response to the fatigue intervention. Indeed, the mean change in the subjects' global efficiency was $\sim 0\%$ without fatigue versus a decrease of $\sim 30\%$ with fatigue.

A secondary hypothesis was that the non-parametric functional muscle network could detect physiological muscle fatigue most particularly in the quadriceps muscles, since they serve as agonists in knee extension and are most active during leg press and play a key role in the sit-to-stand task. Examining the mean non-parametric muscle network in Fig. 1(e) showed a visible decrease in ipsilateral RF-VL on the right side, and in contralateral RF-RF and VL-VL. Moreover, the hypothesis was thoroughly validated in Fig. 4, where all subjects showed a decrease in degree for RF and VL on the right side ($p < 0.001$). The consistent decrease in degree for RF and VL on the non-fatigued side ($p < 0.001$, 13/13 subjects) can be explained by compensation of the contralateral knee extensors.

Additionally, the other ten muscles showed fatigue-related network changes. This observation is despite the fact that these muscles were not directly targeted by the fatiguing task. The consistent decrease in BF on the fatigued side ($p < 0.001$, 13/13 subjects) can be explained by fatigue decreasing the knee flexor's ability to control the descent of sit-to-stand. The change in TA can be attributed to a compensatory mechanism; since RF and VL were fatigued, TA (which is active during sit-to-stand, Fig. 6) may need to provide supplementary control, which could result in deviations from the typical network. In addition, the GO muscle showed a consistent decrease in degree after fatigue, for 12/13 subjects (Fig. 4). An important component of the uniform change in average GO connectivity is its non-parametric coupling with GMAX and GMED. Indeed, both ipsilateral GO-GMED and ipsilateral GO-GMAX decreased post-fatigue for 11/13 subjects on the fatigued side. These results indicate that non-parametric synergistic proximal-distal coupling is diminished after submaximal fatigue is induced in a leg press task. It should be noted that fatigue has been previously shown to effect lower limb joint coupling [93]; thus the reduced hip-ankle muscular coupling here is perhaps indicative of a fatigue-related decrease in the precision of lower limb motor control.

The response of the network indicates the suitability of global analysis of the non-parametric network for detecting fatigue. The consistent decrease in the non-parametric network metrics across muscles is in contrast to recent works based on linear network metrics [63], [64]. Complex, oscillator-based models have been suggested for decoding neural synchronization [94], and non-linear muscle networks have recently decoded the alterations in sensorimotor integration due to stroke [95]. In this paper, the results indicate that non-linear and non-parametric methods are suitable for detecting the neurophysiological phenomenon of fatigue. Macro-connectivity metrics such as global efficiency measure functional integration [74], [81]. Hence, the demonstrated sensitivity (Figs. 2, 3, 7, and 8) of such global metrics as biomarkers of fatigue can be explained by the holistic changes observed throughout the network (Figs. 4, and 5).

The results support the notion that the disruption of motor control induced by fatigue, can result in a systematic response of the proposed non-parametric muscle network. The muscle network response is influenced by subtle functional motor changes and the overall synchronicity of PNS with commands from CNS. The decrease in the connectivity at the muscles targeted by fatigue (shown for the first time in this paper as the primary effect, Figs. 4, 5), can be potentially explained as the reduction in the responsiveness of the fatigued muscles to central commands. The decrease of the connectivity at the other muscles not targeted by fatigue (shown for the first time in this paper as the secondary effect, Figs. 4, 5) may be due to an adaptation mechanism such as compensation or a mirrored biomechanical response. Such an adaptation mechanism would potentially mean that the CNS modulates the control of the other muscles in a synergistically suboptimal and possibly less coordinated manner to conduct the bilateral exercise of sit-to-stand while compensating for the reduction of the natural symmetric response of the fatigued muscles on one side.

It should be noted that the possibility of changes in contralateral control due to fatigue has also been acknowledged in the literature [24], [25], [96]. The fatigue-related decorrelation of the muscle network at both contralateral and ipsilateral levels shows a holistic propagation of synergistic decline at different nodes of the network and the reflection of the decorrelating suboptimal

synergies between the two aforementioned levels. As mentioned, this effect may also be caused by the underlying biomechanical coupling or triggered compensatory mechanisms.

In contrast to the consistent response from the non-parametric muscle network, conventional spectrotemporal methods (RMS, PSD and MDF) showed variable outcomes following volitional submaximal fatigue induced in a leg press task. Inconclusive changes were observed for the average spectrotemporal measurements (Fig. 2(b)). Furthermore, inconsistent patterns of RMS, PSD and MDF were observed for the selected muscles (Fig. 6). The RMS, median PSD, and MDF did not show significant change after fatigue in the targeted muscles (Fig. 6). Therefore, the decrease in network metrics can be attributed to the overall decline in nonlinear and nonparametric synergistic network synchronicity rather than altered amplitude at targeted muscles. The increase in RMS and PSD loosely corresponds to previous studies which found that sEMG activation measurements (RMS) increase in response to fatigue (please note that most existing literature in this regard relates to aerobic fatigue). However, even the aforementioned changes in spectrotemporal measurements do not follow a consistent trend for all subjects. The heterogeneity of the RMS, PSD and MDF results is highlighted by the blue hairlines, which show some subjects showing an increased metric for a given muscle, and other subjects showing no change or even decrease. High inter-subject variability within the results for the established spectrotemporal measurements in response to fatigue tallies with the existing literature [97] and emphasizes the significance of uncovering a robust biomarker of fatigue.

Regarding the broader impact of this work, it can be mentioned that accurate detection of fatigue has strong applications in physiological and rehabilitation settings. The method could be broadly used in exercise sciences, for example measuring individual muscle strength, or a muscle's capacity to work before degradation. Additionally, the muscle group's capability to function correctly in tandem could be monitored, since the non-parametric muscle network identifies fatigue at both the particular muscle and overall network levels. The sub-maximal fatigue that was induced in the participants of this study is also commonly experienced by patients during rehabilitation. Accurate detection of sub-maximal fatigue could optimize clinical rehabilitation programs for various conditions, such as cardiovascular diseases [98], [99] and neuromuscular disorders [100]. Objective quantification of fatigue would represent an improvement on current practices of self-reporting fatigue in current clinical practice [101], where accurate fatigue-tracking could help fatigue management during recovery from conditions such as cancer [102] and other functional motor disorders [103]. The proposed biomarker can help guide rehabilitation from the mentioned disorders, as well as other serious problems which lead to weaker muscles, such as a joint injury or stroke. Accurate monitoring of fatigue could help such patients and therapists to determine when the exercise limit has been reached, and prevent injury potentially caused by continuing. A further rehabilitation application of this method lies in augmented sEMG control of assistive devices. It is known that sEMG signal characteristics change in response to fatigue, and this transformation can affect sEMG-based control of prosthetics and assistive exoskeletons [104]. A precise quantification of fatigue can help such systems to accurately compensate for its effects and maintain their function.

The study is limited by (a) the number of subjects, and (b) not controlling for the variation in ability among the participants. The network biomarker of fatigue was evaluated with 26 subjects, 13 with and 13 without a fatigue intervention. The study did not exclude subjects based on their physical attributes or level of activity. This is done so that the results of the study would be more applicable to the general population. Hence some variations can be expected in physical capabilities across subjects. The future line of research will include a focused analysis of athletic subjects with comparable muscle composition.

V. Conclusion

In this paper, a new modeling technique for decoding the nonlinear synergistic distribution of neural drive at the peripheral nervous system is proposed, namely the non-parametric functional muscle network, and the corresponding efficacy is analyzed as a biomarker of muscle fatigue. Data from 26 subjects (13 in the fatigue intervention group and 13 in the control group) showed that the proposed biomarker could significantly detect fatigue-related decorrelation of the muscle network at the subject level, group level, and node/muscle level. The strong performance of the proposed non-parametric muscle network is accentuated by the observed heterogeneous and inconclusive response of the conventional spectrotemporal measurements of sEMG for detecting fatigue. The proposed fatigue quantification technique has a broad range of applications, most significantly in rehabilitation programs and for motor assessment purposes. The authors would like to highlight that the study was limited by (a) the size of the studied groups of subjects and (b) not controlling for the physical ability of the participants. Future studies would be needed to better understand any compounding factor, such as athletic status. It should be noted that the focus of this study is to propose a new biomarker of fatigue, and the paper has shown that the proposed method can have a superior performance, specifically when classic methods (such as median frequency) fail to detect fatigue consistently.

References

[1] M. Cifrek et al., "Surface EMG based muscle fatigue evaluation in biomechanics," *Clin. Biomech.*, vol. 24, no. 4, pp. 327–340, 2009.
[2] C. J. D. Luca, "Myoelectrical manifestations of localized muscular fatigue in humans," *Crit. Rev. Biomed. Eng.*, vol. 11, no. 4, pp. 251–279, 1984.
[3] R. Merletti, Y. Fan, and R. L. L. Conte, "Estimation of scaling factors in electrically evoked myoelectric signals," in *Proc. 14th Annu. Int. Conf. IEEE Eng. Med. Biol. Soc.*, 1992, vol. 4, pp. 1362–1363.
[4] L. M. Romer and M. I. Polkey, "Exercise-induced respiratory muscle fatigue: Implications for performance," *J. Appl. Physiol.*, vol. 104, no. 3, pp. 879–888, 2008.
[5] R. van den Tillaar and A. Saeterbakken, "Effect of fatigue upon performance and electromyographic activity in 6-RM bench press," *J. Hum. Kinet.*, vol. 40, pp. 57–65, 2014.
[6] S. Jarić et al., "A comparison of the effects of agonist and antagonist muscle fatigue on performance of rapid movements," *Eur. J. Appl. Physiol. Occup. Physiol.*, vol. 76, no. 1, pp. 41–47, 1997.
[7] J. L. Taylor et al., "Changes in muscle afferents, motoneurons and motor drive during muscle fatigue," *Eur. J. Appl. Physiol.*, vol. 83, no. 2, pp. 106–115, 2000.
[8] A. M. Polaski et al., "Exercise-induced hypoalgesia: A meta-analysis of exercise dosing for the treatment of chronic pain," *PLoS one*, vol. 14, no. 1, 2019, Art. no. e0210418.
[9] A. Benjaminse et al., "Revised approach to the role of fatigue in anterior cruciate ligament injury prevention: A systematic review with meta-analyses," *Sports Med.*, vol. 49, no. 4, pp. 565–586, 2019.

[10] B. S. Borotikar et al., "Combined effects of fatigue and decision making on female lower limb landing postures: Central and peripheral contributions to ACL injury risk," *Clin. Biomech.*, vol. 23, no. 1, pp. 81–92, 2008.

[11] M. Liederbach et al., "What is known about the effect of fatigue on injury occurrence among dancers?," *J. Dance Med. Sci.*, vol. 17, no. 3, pp. 101–108, 2013.

[12] S. D. Mair et al., "The role of fatigue in susceptibility to acute muscle strain injury," *Amer. J. Sports Med.*, vol. 24, no. 2, pp. 137–143, 1996.

[13] G. C. Lessi et al., "Comparison of the effects of fatigue on kinematics and muscle activation between men and women after anterior cruciate ligament reconstruction," *Phys. Ther. Sport*, vol. 31, pp. 29–34, 2018.

[14] T. Lowe and X. N. Dong, "The use of hamstring fatigue to reduce quadriceps inhibition after anterior cruciate ligament reconstruction," *Perceptual Motor Skills*, vol. 125, no. 1, pp. 81–92, 2018.

[15] L.-J. Wang et al., "Muscle fatigue enhance beta band EMG-EMG coupling of antagonistic muscles in patients with post-stroke spasticity," *Front. Bioeng. Biotechnol.*, vol. 8, 2020, Art. no. 1007.

[16] M. Bonnard et al., "Different strategies to compensate for the effects of fatigue revealed by neuromuscular adaptation processes in humans," *Neurosci. Lett.*, vol. 166, no. 1, pp. 101–105, 1994.

[17] A.-F. Huffenus et al., "Effects of distal and proximal arm muscles fatigue on multi-joint movement organization," *Exp. Brain Res.*, vol. 170, no. 4, pp. 438–447, 2006.

[18] J. N. Côté et al., "Movement reorganization to compensate for fatigue during sawing," *Exp. Brain Res.*, vol. 146, no. 3, pp. 394–398, 2002.

[19] M. Kouzaki et al., "Alternate muscle activity observed between knee extensor synergists during low-level sustained contractions," *J. Appl. Physiol.*, vol. 93, no. 2, pp. 675–684, 2002.

[20] P. V. Komi and P. Tesch, "EMG frequency spectrum, muscle structure, and fatigue during dynamic contractions in man," *Eur. J. Appl. Physiol. Occup. Physiol.*, vol. 42, no. 1, pp. 41–50, 1979.

[21] L. R. Brody et al., "pH-induced effects on median frequency and conduction velocity of the myoelectric signal," *J. Appl. Physiol.*, vol. 71, no. 5, pp. 1878–1885, 1991.

[22] M. Lévénez et al., "Spinal reflexes and coactivation of ankle muscles during a submaximal fatiguing contraction," *J. Appl. Physiol.*, vol. 99, no. 3, pp. 1182–1188, 2005.

[23] S. Baudry et al., "Age-related fatigability of the ankle dorsiflexor muscles during concentric and eccentric contractions," *Eur. J. Appl. Physiol.*, vol. 100, no. 5, pp. 515–525, 2007.

[24] T. J. Carroll et al., "Contralateral effects of unilateral strength training: Evidence and possible mechanisms," *J. Appl. Physiol.*, vol. 101, no. 5, pp. 1514–1522, 2006.

[25] N. Hedayatpour et al., "The effect of eccentric exercise and delayed onset muscle soreness on the homologous muscle of the contralateral limb," *J. Electromyogr. Kinesiol.*, vol. 41, pp. 154–159, 2018.

[26] M. González-Izal et al., "Electromyographic models to assess muscle fatigue," *J. Electromyogr. Kinesiol.*, vol. 22, no. 4, pp. 501–512, 2012.

[27] H. A. Yousif et al., "Assessment of muscles fatigue based on surface EMG signals using machine learning and statistical approaches: A review," in *Proc. IOP Conf. Ser.: Mater. Sci. Eng.*, 2019, vol. 705, no. 1, Art. no. 012010.

[28] S. Rampichini et al., "Complexity analysis of surface electromyography for assessing the myoelectric manifestation of muscle fatigue: A review," *Entropy*, vol. 22, no. 5, pp. 1–31, 2020.

[29] C. J. D. Luca, "Physiology and mathematics of myoelectric signals," *IEEE Trans. Biomed. Eng.*, vol. 26, no. 6, pp. 313–325, Jun. 1979.

[30] R. Merletti and P. J. Parker, *Electromyography: Physiology, Engineering, and Non-Invasive Applications*. Hoboken, NJ, USA: Wiley, 2004.

[31] F. Menotti et al., "Neuromuscular function after muscle fatigue in charcot–marie–tooth type 1A patients," *Muscle Nerve*, vol. 46, no. 3, pp. 434–439, 2012.

[32] W. Guo, X. Sheng, and X. Zhu, "Assessment of muscle fatigue by simultaneous sEMG and NIRS: From the perspective of electrophysiology and hemodynamics," in *Proc. 8th Int. IEEE/EMBS Conf. Neural Eng.*, 2017, pp. 33–36.

[33] P. A. Tesch et al., "Force and EMG signal patterns during repeated bouts of concentric or eccentric muscle actions," *Acta Physiol. Scand.*, vol. 138, no. 3, pp. 263–271, 1990.

[34] T. Moritani et al., "Intramuscular and surface electromyogram changes during muscle fatigue," *J. Appl. Physiol.*, vol. 60, no. 4, pp. 1179–1185, 1986.

[35] L. Arendt-Nielsen and K. R. Mills, "Muscle fibre conduction velocity, mean power frequency, mean EMG voltage and force during submaximal fatiguing contractions of human quadriceps," *Eur. J. Appl. Physiol. Occup. Physiol.*, vol. 58, no. 1–2, pp. 20–25, 1988.

[36] M. Bilodeau et al., "EMG frequency content changes with increasing force and during fatigue in the quadriceps femoris muscle of men and women," *J. Electromyogr. Kinesiol.*, vol. 13, no. 1, pp. 83–92, 2003.

[37] L. Wang et al., "A comparative study of EMG indices in muscle fatigue evaluation based on grey relational analysis during all-out cycling exercise," *Biomed. Res. Int.*, vol. 2018, 2018, Art. no. 9341215.

[38] J. L. Dideriksen et al., "An integrative model of motor unit activity during sustained submaximal contractions," *J. Appl. Physiol.*, vol. 108, no. 6, pp. 1550–1562, 2010.

[39] J. L. Dideriksen et al., "Influence of fatigue on the simulated relation between the amplitude of the surface electromyogram and muscle force," *Philos. Trans. A. Math. Phys. Eng. Sci.*, vol. 368, no. 1920, pp. 2765–2781, 2010.

[40] K. Masuda et al., "Changes in surface EMG parameters during static and dynamic fatiguing contractions," *J. Electromyogr. Kinesiol.*, vol. 9, no. 1, pp. 39–46, 1999.

[41] M. Naeije and H. Zorn, "Relation between EMG power spectrum shifts and muscle fibre action potential conduction velocity changes during local muscular fatigue in man," *Eur. J. Appl. Physiol. Occup. Physiol.*, vol. 50, no. 1, pp. 23–33, 1982.

[42] L. Arendt-Nielsen and T. Sinkjær, "Quantification of human dynamic muscle fatigue by electromyography and kinematic profiles," *J. Electromyogr. Kinesiol.*, vol. 1, no. 1, pp. 1–8, 1991.

[43] W. Ament et al., "Electromyogram median power frequency in dynamic exercise at medium exercise intensities," *Eur. J. Appl. Physiol. Occup. Physiol.*, vol. 74, no. 1–2, pp. 180–186, 1996.

[44] T. J. Carroll et al., "Recovery of central and peripheral neuromuscular fatigue after exercise," *J. Appl. Physiol.*, vol. 122, no. 5, pp. 1068–1076, 2017.

[45] J. Zeng, Y. Zhou, Y. Yang, J. Yan, and H. Liu, "Fatigue-sensitivity comparison of sEMG and A-Mode ultrasound based hand gesture recognition," *IEEE J. Biomed. Health Inform.*, vol. 26, no. 4, pp. 1718–1725, Oct. 2022.

[46] Z. Sheng, N. Sharma, and K. Kim, "Quantitative assessment of changes in muscle contractility due to fatigue during NMES: An ultrasound imaging approach," *IEEE Trans. Biomed. Eng.*, vol. 67, no. 3, pp. 832–841, Mar. 2020.

[47] S. Wang, H. Tang, B. Wang, and J. Mo, "A novel approach to detecting muscle fatigue based on sEMG by using neural architecture search framework," *IEEE Trans. Neural Netw. Learn. Syst.*, early access, Nov. 9, 2021, doi: 10.1109/TNNLS.2021.3124330.

[48] B. Zhou et al., "Electrical impedance myography for evaluating muscle fatigue induced by neuromuscular electrical stimulation," *IEEE J. Electromagn., RF, Microw. Med. Biol.*, vol. 6, no. 1, pp. 94–102, Mar. 2022.

[49] K. B. Smale et al., "Use of muscle synergies and wavelet transforms to identify fatigue during squatting," *J. Electromyogr. Kinesiol.*, vol. 28, pp. 158–166, 2016.

[50] T. Singh and M. L. Latash, "Effects of muscle fatigue on multi-muscle synergies," *Exp. Brain Res.*, vol. 214, no. 3, pp. 335–350, 2011.

[51] P. A. Ortega-Auriol et al., "Fatigue influences the recruitment, but not structure, of muscle synergies," *Front. Hum. Neurosci.*, vol. 12, 2018, Art. no. 217.

[52] V. C. K. Cheung et al., "Stability of muscle synergies for voluntary actions after cortical stroke in humans," *Proc. Nat. Acad. Sci. USA*, 2009, vol. 106, no. 46, pp. 19563–19568.

[53] M. C. Tresch and A. Jarc, "The case for and against muscle synergies," *Curr. Opin. Neurobiol.*, vol. 19, no. 6, pp. 601–607, 2009.

[54] Y. Wang et al., "Aging effect on muscle synergies in stepping forth during a forward perturbation," *Eur. J. Appl. Physiol.*, vol. 117, no. 1, pp. 201–211, 2017.

[55] A. Sawers et al., "Long-term training modifies the modular structure and organization of walking balance control," *J. Neurophysiol.*, vol. 114, no. 6, pp. 3359–3373, 2015.

[56] J. L. Allen et al., "Increased neuromuscular consistency in gait and balance after partnered, dance-based rehabilitation in parkinson's disease," *J. Neurophysiol.*, vol. 118, no. 1, pp. 363–373, 2017.

[57] J. Xu et al., "Network theory based EHG signal analysis and its application in preterm prediction," *IEEE J. Biomed. Health Informat.*, vol. 26, no. 7, pp. 2876–2887, Jul. 2022.

[58] N. Nader et al., "Graph analysis of uterine networks using EHG source connectivity," in *Proc. 4th Int. Conf. Adv. Biomed. Eng.*, 2017, pp. 1–4.

[59] J. N. Kerkman et al., "Network structure of the human musculoskeletal system shapes neural interactions on multiple time scales," *Sci. Adv.*, vol. 4, no. 6, 2018, Art. no. eaat0497.

[60] A. Del Vecchio et al., "The human central nervous system transmits common synaptic inputs to distinct motor neuron pools during non-synergistic digit actions," *J. Physiol.*, vol. 597, no. 24, pp. 5935–5948, 2019.

[61] T. W. Boonstra et al., "Muscle networks: Connectivity analysis of EMG activity during postural control," *Sci. Rep.*, vol. 5, no. 1, pp. 1–14, 2015.

[62] T. W. Boonstra et al., "Information decomposition of multichannel EMG to map functional interactions in the distributed motor system," *NeuroImage*, vol. 202, 2019, Art. no. 116093.

[63] C. Charissou et al., "Fatigue-and training-related changes in 'beta' intermuscular interactions between agonist muscles," *J. Electromyogr. Kinesiol.*, vol. 27, pp. 52–59, 2016.

[64] P. C. R. Dos Santos et al., "Age-specific modulation of intermuscular beta coherence during gait before and after experimentally induced fatigue," *Sci. Rep.*, vol. 10, no. 1, pp. 1–12, 2020.

[65] B. A. Alkner et al., "Quadriceps EMG/force relationship in knee extension and leg press," *Med. Sci. Sports Exerc.*, vol. 32, no. 2, pp. 459–463, 2000.

[66] K. Bouillard et al., "Effect of vastus lateralis fatigue on load sharing between quadriceps femoris muscles during isometric knee extensions," *J. Neurophysiol.*, vol. 111, no. 4, pp. 768–776, 2014.

[67] H. S. Al Amer et al., "Electromyographic activity of quadriceps muscle during sit-to-stand in patients with unilateral knee osteoarthritis," *BMC Res. Notes*, vol. 11, no. 1, pp. 1–6, 2018.

[68] V. Ferreira et al., "Biomechanics performance in 30-S chair stand test in patients with medial knee osteoarthritis," *Int. J. Hum. Factors Ergonom.*, vol. 6, no. 4, pp. 319–330, 2019.

[69] R. W. Bohannon, "Knee extension strength and body weight determine sit-to-stand independence after stroke," *Physiother. Theory Pract.*, vol. 23, no. 5, pp. 291–297, 2007.

[70] O. Eriksrud and R. W. Bohannon, "Relationship of knee extension force to independence in it-to-stand performance in patients receiving acute rehabilitation," *Phys. Ther.*, vol. 83, no. 6, pp. 544–551, 2003.

[71] A. Aguirre et al., "Machine learning approach for fatigue estimation in sit-to-stand exercise," *Sensors*, vol. 21, no. 15, 2021, Art. no. 5006.

[72] F. Bahrami et al., "Biomechanical analysis of Sit-to-stand transfer in healthy and paraplegic subjects," *Clin. Biomech.*, vol. 15, no. 2, pp. 123–133, 2000.

[73] J. L. Helbostad et al., "Consequences of lower extremity and trunk muscle fatigue on balance and functional tasks in older people: A systematic literature review," *BMC Geriatr.*, vol. 10, 2010, Art. no. 56.

[74] M. Rubinov and O. Sporns, "Complex network measures of brain connectivity: Uses and interpretations," *Neuroimage*, vol. 52, no. 3, pp. 1059–1069, 2010.

[75] D. J. Watts and S. H. Strogatz, "Collective dynamics of 'small-world' networks," *Nature*, vol. 393, no. 6684, pp. 440–442, 1998.

[76] I. H. Bruun et al., "Validity and responsiveness to change of the 30-Second chair-stand test in older adults admitted to an emergency department," *J. Geriatr. Phys. Ther.*, vol. 42, no. 4, pp. 265–274, 2019.

[77] B. Unver et al., "Test-retest reliability of the 50-foot timed walk and 30-Second chair stand test in patients with total hip arthroplasty," *Acta Orthop. Belg.*, vol. 81, no. 3, pp. 435–841, 2015.

[78] G. C. Bogdanis et al., "Comparison between unilateral and bilateral plyometric training on Single-and double-leg jumping performance and strength," *J. Strength Conditioning Res.*, vol. 33, no. 3, pp. 633–640, 2019.

[79] C. Latella et al., "Reduction in corticospinal inhibition in the trained and untrained limb following unilateral LEG strength training," *Eur. J. Appl. Physiol.*, vol. 112, no. 8, pp. 3097–3107, 2012.

[80] J. Saramäki et al., "Generalizations of the clustering coefficient to weighted complex networks," *Phys. Rev. E. Statist. Nonlin. Soft Matter Phys.*, vol. 75, no. 2,2007, Art. no. 027105.

[81] V. Latora and M. Marchiori, "Efficient behavior of small-world networks," *Phys. Rev. Lett.*, vol. 87, no. 19, 2001, Art. no. 198701.

[82] A. Phinyomark et al., "Surface electromyography (EMG) signal processing, classification, and practical considerations," in *Biomedical Signal Processing: Advances in Theory, Algorithms and Applications*, G. Naik, Ed. Berlin, Germany: Springer, 2020, pp. 3–29.

[83] R. Merletti and G. L. Cerone, "Tutorial. surface EMG detection, conditioning and pre-processing: Best practices," *J. Electromyogr. Kinesiol.*, vol. 54, 2020, Art. no. 102440.

[84] C. J. D. Luca et al., "Filtering the surface EMG signal: Movement artifact and baseline noise contamination," *J. Biomech.*, vol. 43, no. 8, pp. 1573–1579, 2010.

[85] O. P. Neto and E. A. Christou, "Rectification of the EMG signal impairs the identification of oscillatory input to the muscle," *J. Neurophysiol.*, vol. 103, no. 2, pp. 1093–1103, 2010.

[86] J. F. Yang and D. A. Winter, "Electromyographic amplitude normalization methods: Improving their sensitivity as diagnostic tools in gait analysis," *Arch. Phys. Med. Rehabil.*, vol. 65, no. 9, pp. 517–521, 1984.

[87] A. Burden, "How should we normalize electromyograms obtained from healthy participants? What we have learned from over 25 years of research," *J. Electromyogr. Kinesiol.*, vol. 20, no. 6, pp. 1023–1035, 2010.

[88] M. Besomi et al., "Consensus for experimental design in electromyography (CEDE) project: Amplitude normalization matrix," *J. Electromyogr. Kinesiol.*, vol. 53, 2020, Art. no. 102438.

[89] M. B. Lanza et al., "Normalization of the electromyography amplitude during a multiple-set resistance training protocol: Reliability and differences between approaches," *J. Electromyogr. Kinesiol.*, vol. 68, 2022, Art. no. 102724.

[90] A. Chalard et al., "Impact of the EMG normalization method on muscle activation and the antagonist-agonist co-contraction index during active elbow extension: Practical implications for post-stroke subjects," *J. Electromyogr. Kinesiol.*, vol. 51, 2020, Art. no. 102403.

[91] D. A. Winter and H. J. Yack, "EMG profiles during normal human walking: Stride-to-stride and inter-subject variability," *Electroencephalogr. Clin. Neurophysiol.*, vol. 67, no. 5, pp. 402–411, 1987.

[92] A. M. Burden et al., "Normalisation of gait EMGs: A re-examination," *J. Electromyogr. Kinesiol.*, vol. 13, no. 6, pp. 519–532, 2003.

[93] J. H. Hollman et al., "Hip extensor fatigue alters hip and knee coupling dynamics during single-limb step-downs: A randomized controlled trial," *J. Biomech.*, vol. 100, 2020, Art. no. 109583.

[94] R. G. Erra et al., "Neural synchronization from the perspective of nonlinear dynamics," *Front. Comput. Neurosci.*, vol. 11, 2017, Art. no. 98.

[95] R. O'Keeffe et al., "Nonlinear functional muscle network based on information theory tracks sensorimotor integration post stroke," *Sci. Rep.*, vol. 12, no. 1, Jul. 2022, Art. no. 13029.

[96] N.-P. Brøchner Nielsen et al., "Motor adaptations to unilateral quadriceps fatigue during a bilateral pedaling task," *Scand. J. Med. Sci. Sports*, vol. 27, no. 12, pp. 1724–1738, 2017.

[97] B. Gerdle et al., "Criterion validation of surface EMG variables as fatigue indicators using peak torque: A study of repetitive maximum isokinetic knee extensions," *J. Electromyogr. Kinesiol.*, vol. 10, no. 4, pp. 225–232, 2000.

[98] P. Kligfield et al., "Effect of age and gender on heart rate recovery after submaximal exercise during cardiac rehabilitation in patients with angina pectoris, recent acute myocardial infarction, or coronary bypass surgery," *Amer. J. Cardiol.*, vol. 92, no. 5, pp. 600–603, 2003.

[99] J. L. Reed et al., "Submaximal exercise testing in cardiovascular rehabilitation settings (BEST study)," *Front. Physiol.*, vol. 10, 2019, Art. no. 1517.

[100] D. L. Turner et al., "Recovery of submaximal upper limb force production is correlated with better arm position control and motor impairment early after a stroke," *Clin. Neurophysiol.*, vol. 123, no. 1, pp. 183–192, 2012.

[101] C. O'Connell and E. K. Stokes, "Fatigue–concepts for physiotherapy management and measurement," *Phys. Ther. Rev.*, vol. 12, no. 4, pp. 314–323, 2007.

[102] C. M. Donnelly et al., "Physiotherapy management of cancer-related fatigue: A survey of UK current practice," *Supportive Care Cancer*, vol. 18, no. 7, pp. 817–825, 2010.

[103] G. Nielsen et al., "Physiotherapy for functional motor disorders: A consensus recommendation," *J. Neurol., Neurosurg. Psychiatry*, vol. 86, no. 10, pp. 1113–1119, 2015.

[104] T. D. Lalitharatne, Y. Hayashi, K. Teramoto, and K. Kiguchi, "A study on effects of muscle fatigue on EMG-based control for human upper-limb power-assist," in *Proc. IEEE 6th Int. Conf. Inf. Automat. Sustainability*, 2012, pp. 124–128.